Ternary Fission of Uranium-236* and -234*†

M. L. MUGA, C. R. RICE,* AND W. A. SEDLACEK‡
Department of Chemistry and Department of Physics, The University of Florida, Gainesville, Florida
(Received 18 May 1967)

A detailed study of the ternary fission of U^{236*} and U^{234*} has been completed using a triple-coincidence technique and a three-parameter energy measurement on the product fragments. Arguments based on experimental energy, angular, and frequency correlations are presented for elimination of phenomena other than ternary fission as explanations of the observed data. Among possible interfering effects considered were (1) accidental events, (2) instrumental malfunctions, and (3) scattering phenomena. In connection with the third factor, an experimental determination of the characteristics of binary-fission-fragment scattering confirmed the absence of this phenomenon from all but one of the angular arrangements investigated. It is concluded that the major portion of triple events observed arises from a ternary-fission process. A difference in the ternary-fission properties of U^{236*} and U^{234*} is interpreted as caused by the dominant effect of underlying shell structure in forming the product fragments, an effect which may result in the formation of unique (preselected) fragments masses. Mass distributions indicate the formation of low-mass fission products with mass peaks centered near 30 and 50 amu. A qualitative mechanism by which the ternary-fission process may occur is presented.

I. INTRODUCTION

INVESTIGATION of the fission of heavy nuclei into three large fragments of comparable size has seen a revived interest in recent years. Both nuclear emulsion techniques and instrumental methods give evidence for the existence of this rare mode of nuclear division.[1] Refinements in instrumental techniques have furthermore resulted in the measurement of approximate mass distributions from ternary fission.[2,3] In attempts to detect light mass fragments, radiochemical methods[4–6] have set upper limits for the yield of mass chains 28, 38, 39, 41, 42, 49, 56, and 59 which are too low to be consistent with the frequency indicated by instrumental techniques. Shielded or neutron deficient nuclides at masses 37, 48, 51, 54, 56, 57, 58, and 60 were also examined. These results eliminate eight out of approximately forty low-mass chains in question but do not preclude the possibility of unique mass formation in the ternary-fission process.

On the more positive side, production of Si^{32} activity has been associated with high altitude nuclear weapons testing.[7] It is not clear whether this activity could be produced by a double (n,p) reaction on sulphur-32 in the device components or by thermonuclear processes such as occurs in stars (other processes were ruled out as unlikely). However, the estimated production ($\sim 10^{-4}$ per binary fission) is not inconsistent with an explanation based on ternary fission induced by fast neutrons.

The failure of radiochemical attempts[4–6] to confirm these results has focused added attention on this process by questioning the validity of the instrumental results. Re-evaluation of these results, however, has made it abundantly clear that the data cannot be merely disregarded by attributing them to spurious events. In an effort to resolve this apparent discrepancy we have completed a rather exhaustive study, using instrumental methods, of the thermal-neutron-induced ternary fission of the uranium isotopes 235 and 233.

II. EXPERIMENTAL

The procedure involves the detection and parallel energy measurement of the three fragments resulting from tripartition. The experimental arrangement is essentially that described in Ref. 3 and shown, drawn to scale, in Fig. 1. Three solid state detectors were placed at chosen angles and at a fixed distance in a plane about a fission source. Signals from these detectors were routed to a three-coincident-parameter analyzer having 256×256×256-channel resolution.

A. Apparatus

The detectors were of the surface-barrier type fabricated from 300 Ω cm silicon with a sensitive area of not greater than 0.25 cm² (5mm×5mm). Normally, the detectors were operated at 30-V back-bias voltage and were replaced before the back-bias current exceeded 10 μA. In order to maintain a constant depletion depth during the course of an irradiation, periodic adjustments (in increments of 2 V) of the back-bias voltage were made as the back-bias current increased.

The radial positions of the detectors were fixed at 1.0, 1.5, or 2.0 cm corresponding to subtended solid angles of 0.25, 0.11, and 0.063 sr (and planar angles of

† Work supported by the U. S. Atomic Energy Commission through contract AT (40-1)-2843. Report ORO-2843-10.
* Chemistry Department, Florida College, Temple Terrace, Florida.
‡ Present address: Los Alamos Scientific Laboratory, University of California, Los Alamos, New Mexico.
[1] A review of the history of the earlier work appears in E. Hyde, *Nuclear Properties of the Heavy Elements*. (Prentice-Hall, Inc., Englewood Cliffs, New Jersey, 1964), Vol. 3, p. 131.
[2] M. L. Muga, Phys. Rev. Letters **11**, 129 (1963).
[3] M. L. Muga, in *Proceedings of the Symposium on Physics and Chemistry of Fission*, (International Atomic Energy Agency, Vienna, 1965), Vol. II, paper SM-60/73, p. 409.
[4] R. W. Stoenner and M. Hillman, Phys. Rev. **142**, 716 (1966); Abstract J14, 151st ACS Meeting, Pittsburgh, March, 1966 (unpublished).
[5] R. J. Prestwood and B. P. Bayhurst, Abstract J15, 151st ACS Meeting, Pittsburgh, March, 1966 (unpublished).
[6] J. C. Roy, Can. J. Phys. **39**, 315 (1961).
[7] W. Dansgaard, H. B. Clausen, and A. Aarkrog, J. Geophys. Res. **71**, 5474 (1966).

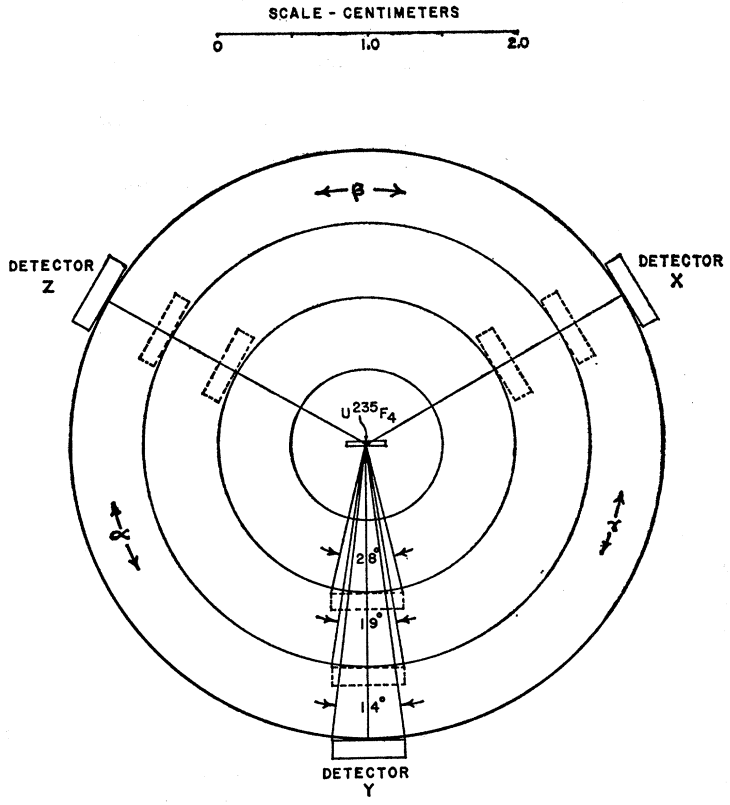

FIG. 1. Scale drawing of experimental configuration used for ternary-fission studies.

28, 19, and 14 deg), respectively. The choice of the radial and angular position was guided by the goal of each particular experiment, viz., better angular resolution was achieved for the 2.0-cm radial position but with a sacrifice in numbers of events recorded in a typical experiment. The angular positions of two detectors (X and Z) could be adjusted and monitored by external controls.

The uranium sources of uniform thickness were prepared by slowly evaporating (in vacuum) UF_4 onto (10—20 $\mu g/cm^2$) VYNS film supported on thin (0.025 cm) nickel washers. The uranium (IV) fluoride deposit was confined to a circular area 0.282 cm in diameter by a collimating system. Sources ranging up to 5×10^{-4} g/cm^2 thickness (as determined by alpha-particle counting at known geometry and, independently, by alpha-particle energy-degradation methods) were fabricated. The sources were mounted parallel to the surface of the stationary Y detector, the uranium side facing away.

The uranium isotopes were obtained from the Oak Ridge National Laboratories and had the composition indicated in Table I.

The detectors and source were enclosed in an evacuated aluminum chamber (see Fig. 2 of Ref. 3), which in turn was placed in the thermal column (intercepting a flux of approximately 10^{10} n/cm^2 sec) of the University of Florida Training Reactor (UFTR). The epicadmium to thermal neutron ratio at the irradiation site is approximately 1:10.

B. Electronics

The schematic of the basic electronic recording system is shown in Fig. 2(a), (b). The output from each of three solid-state detectors is amplified by "Nuvistorized"[7a] preamplifiers and is paralleled to two amplifier systems, one of which (linear or slow amplifier) conserves linear response of the detector pulse; the other (fast amplifier) preserves a fast rise time. The latter pulse is directed to a fast discriminator and pulse shaper which delivers a 5–120-nsec wide pulse (preselected) that is applied to a three-fold fast coincidence circuit. The discriminator was set just above the noise level in each of the fast pulse circuits. The triple coincidence output serves to

TABLE I. Composition of isotopes obtained from the Oak Ridge National Laboratories.

U^{235}		U^{233}	
Mass No.	%	Mass No.	%
234	0.038	233	99.541
235	99.909	234	0.032
236	none detectable	235	0.021
238	0.053	236	0.001
		238	0.405

[7a] The use of miniature RCA Nuvistor tubes was prompted by space considerations and the fact that transistorized preamplifiers deteriorated rapidly in the reactor neutron flux.

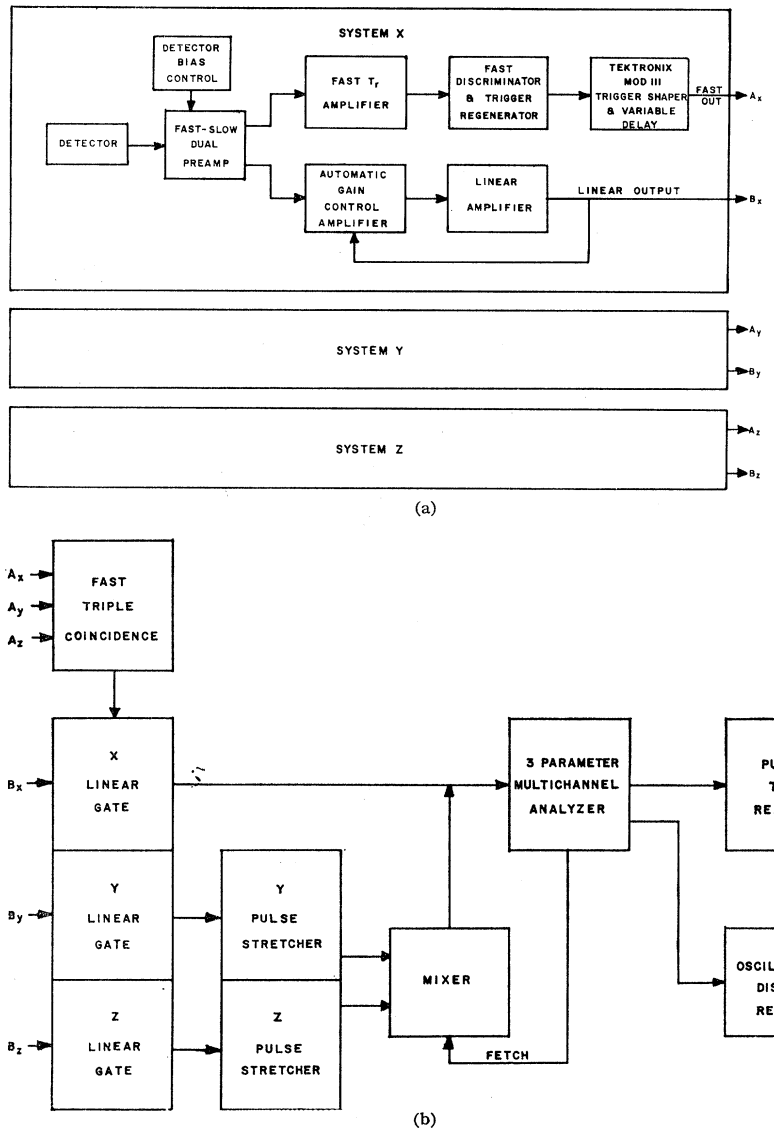

FIG. 2. Schematic diagram of electronic recording system capable of three-parameter multichannel analysis.

open three linear gates, allowing the outputs of the three linear amplifiers to pass through for subsequent analysis. One pulse is immediately analyzed; the other two pulses are temporarily stored in the buffer storage (pulse stretcher) unit from which they are sequentially released on command and analyzed. Upon completion of this three-stage digital conversion, automatic readout on punched paper tape is achieved.

Autogain stabilizers were incorporated into the linear amplifier systems using the energy position of the light-mass binary-fission fragment for reference. Calibration of the detectors was achieved by recording the binary-fission fragment kinetic-energy spectrum before and after the experiment. Typically, during an experiment no gain shift of the reference peak was observed; the energy peak of the heavy fragment usually shifted upward some two to four channel numbers (1–2 MeV) during a 5-h run. Background effects were few, and when present could be traced to poor settings of the fast-pulse discriminator and/or to line-voltage transients caused by nearby construction crews. In any event, identification of this "noise" was made on the basis of the accompanying energy analysis of the three linear pulses as described next.

C. Data Reduction

In the reduction process, events for which any one detector registered less than 16 channel numbers were discarded. It was estimated that long-range α particles (from the fission process) saturated the detector depletion layer with pulse heights corresponding to 14 channel numbers or less, and hence their interference was removed. Events caused by background effects were likewise discarded.

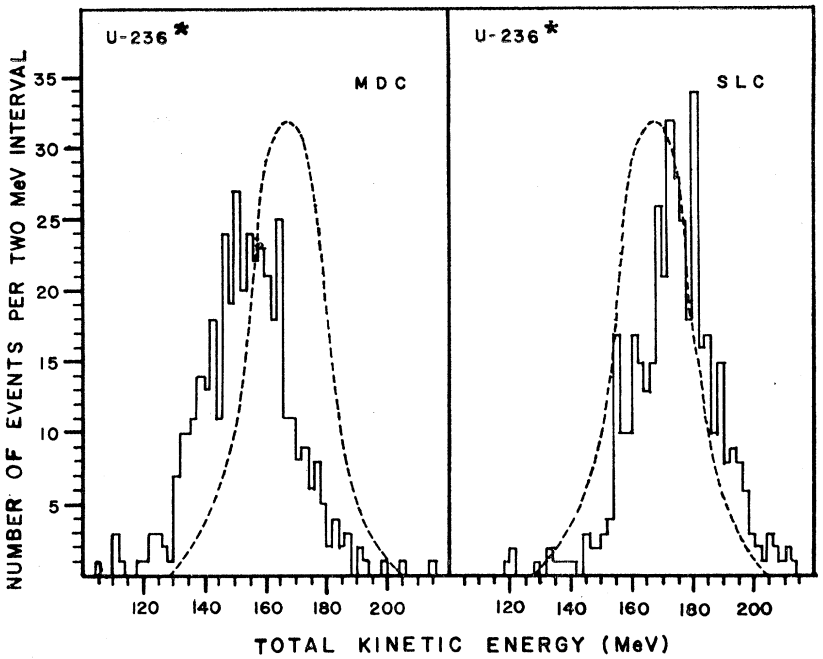

FIG. 3. Total fragment kinetic-energy distribution for U^{236*} system showing effect of calibration schemes SLC and MDC (see text). Dashed line represents total kinetic-energy release for binary fission. Data taken with detectors at 1.5 cm distance from source.

The following three methods were used for converting raw data to energy dimensions.

(a) Straight-line calibration (SLC)—The binary fission fragment spectra were compared with that from time-of-flight data[8,9] and linear extrapolation to lower energies was made using the average light- and heavy-mass energy positions.

(b) Mass-dependent calibration (MDC)—The linear-mass-dependent method described by Schmitt *et al.*[10] was applied after first obtaining approximate masses based on the SLC approach.[11] A new set of masses was then computed and the process repeated until the energy values converged to within 0.5 MeV.

(c) Quadratic mass-dependent calibration (QMDC)—*A* quadratic mass-dependent method (described in the appendix) was applied in the same manner as the MDC method above.

The latter two methods gave results substantially the same, but which were quite different from those obtained from the SLC approach. It is felt that these latter two methods give more reliable values than the first.

[8] J. C. D. Milton and J. S. Fraser, Can. J. Phys. 40, 1626 (1962).
[9] J. S. Fraser, J. C. D. Milton, H. R. Bowman, and S. G. Thompson, Can. J. Phys. 41, 2080 (1963).
[10] H. W. Schmitt, W. M. Gibson, J. H. Neiler, F. J. Walter, and T. D. Thomas, in *Proceedings of the Symposium on the Physics and Chemistry of Fission* (International Atomic Energy Agency, Vienna, 1965), Vol. I, paper SM-60/40, p. 531; and private communication.
[11] The following relation was used:

$$m_i = \frac{M \sin^2\theta_i}{(E_i/E_1)\sin^2\theta_1 + (E_i/E_2)\sin^2\theta_2 + (E_i/E_3)\sin^2\theta_3}$$

where m_i is the mass of ith fragment, $i=1,2,3,$; E_i is the energy of ith fragment; θ_1 is the angle between fragments 2 and 3; θ_2 is the angle between fragments 1 and 3; θ_3 is the angle between fragments 2 and 1; M is the mass of fissioning nucleus.

Single count rates were typically 2000–5000 counts/sec. Under these conditions, data could be collected for up to 6–8 h after which a very rapid deterioration (especially, in the fast pulse rise time) of the detectors was observed. For the most part, this deterioration appeared to result primarily from the fission fragment flux rather than from the γ and fast-neutron flux in the UFTR thermal column.

III. RESULTS AND DISCUSSION

In this section, energy distributions are presented followed by a discussion of the possible causes of triple events. Finally, the mass distributions and interpretation are given.

Triple events were recorded at different angular positions and for subtended planar angles of 28°, 19°, and 14° (see Fig. 1). The angular arrangements are referred to in the following text as (120-120-120), (130-100-130) and (140-80-140), the three numbers in each parenthesis corresponding, respectively, to the three angles α, β, and γ defined in Fig. 1.

A. Kinetic Energy and Frequency of Occurrence

The total fragment kinetic energy released in ternary fission (TF) of U^{236*} and U^{234*} is shown, respectively, in Figs. 3 and 4. The detector positions are symmetric about the source ($\alpha=\beta=\gamma=120°$). The effect caused by the use of different calibration schemes is readily apparent; the plot resulting from applying the quadratic mass-dependent calibration (QMDC) is essentially identical with that for the mass-dependent calibration (MDC) and is not shown. Average values for the total fragment kinetic-energy release are shown in Table II.

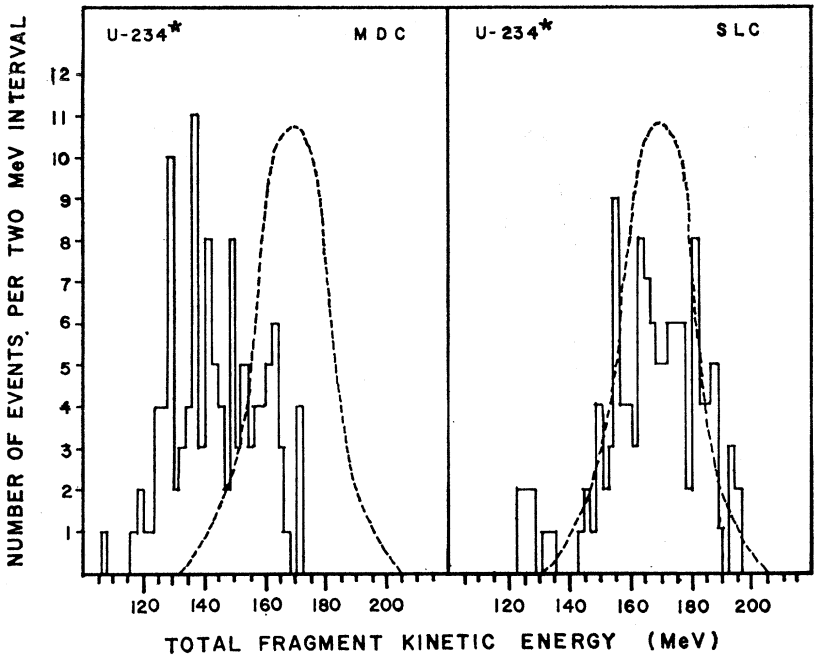

FIG. 4. Total fragment kinetic-energy distribution for U^{234*} system showing effect of calibration schemes SLC and MDC (see text). Dashed line represents total kinetic-energy release for binary fission. Data taken with detectors at 1.5-cm distance from source.

The average total kinetic energy released for different angular arrangements is listed in Table III. The mass-dependent calibration indicates a *kinetic energy* release substantially lower than that for binary fission.

The single-fragment energy spectra are shown in Figs. 5 and 6. Again, the effect of different calibration procedures is evident; the mass-dependent calibrations generally give lower energies. A breakdown of the range of low-, median-, and high-energy fragments for the system ($U^{235}+n_{th} \rightarrow$ T.F.) is shown in Figs. 7 and 8. For ease of comparison events have been classified into types I and II on the basis suggested by previous work.[3] (See also Sec. III D following.)

The variations of single-fragment energy distributions with different angular arrangements of the detectors are shown in Fig. 9 for the U^{236*} system. Distinct variations in the shapes are apparent, notably, the disappearance [as two detectors (X and Y) are placed closer to each other] of fragments having energies in the range of the low-energy binary fission fragments. Also, we note the formation of two low-energy peaks for the detector arrangement ($\alpha=130°$, $\beta=100°$, $\gamma=130°$), an arrangement for which scattering phenomena may contribute significantly (see Sec. IIIC).

The frequency of the triple-event count rate relative to the single count rates of binary-fission fragments is shown in Table IV for various detector arrangements.

TABLE II. Average total fragment kinetic energies in MeV from ternary fission as obtained using different calibration schemes. Detector angles are $\alpha=\beta=\gamma=120°$. SLC, MDC, and QMDC refer to calibration procedures as explained in text. Errors shown are average errors based on differences in average total kinetic energies from different data sets.

Fissioning system	Binary fission	SLC	MDC	QMDC
$U^{233}+n_{th}$	167.8	168±4	144±4	···
$U^{235}+n_{th}$	168.2	175±4	155±5	155±5

TABLE III. Average total kinetic-energy release in MeV from ternary fission of U^{236*} system. Subtended planar angle equals 19°. SLC, MDC, and QMDC refer to calibration procedures as explained in text. Errors shown are average errors based on differences in average total kinetic energies from different data sets.

Detector configuration α β γ	Calibration method SLC	MDC	QMDC
140- 80-140	182±2	162±1	···
130-100-130	176±3	156±3	···
120-120-120	175±4	155±5	155±5

TABLE IV. Average frequency of occurrence of triple-fission (TF) events relative to binary-fission (BF) events corrected for geometrical efficiency. Values shown may be taken as lower limits. Errors shown reflect statistical errors of counting.

Angular arrangement α - β - γ	Distance from source in cm[a]	10^6(TF/BF) U^{236*}	U^{234*}
120-120-120	1.0	28±2	26±2
	1.5	7±2	15±2
	2.0	2±1	6±1
130-100-130	1.0	21±3	···
	1.5	10±2	7±2
	2.0	9±3	5±2
140- 80-140	1.5	2±1	2±1
	2.0	1[b]	0[c]
110-140-110	2.0	8±3	7±2

[a] For 5mm×5mm detector; see Fig. 1.
[b] Based on one event obtained in one experimental run.
[c] Based on zero events obtained in two experimental runs.

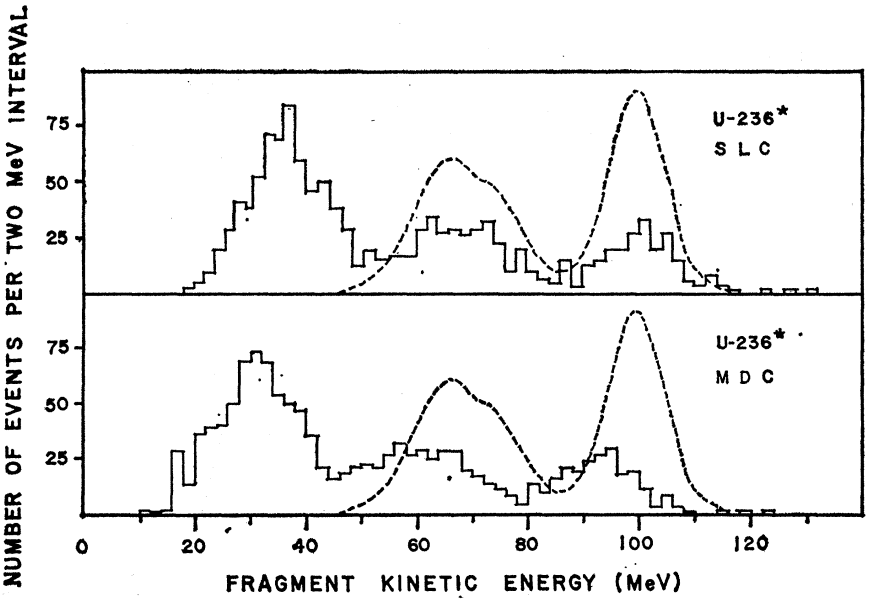

FIG. 5. Single fragment kinetic-energy distribution for U^{236*} system showing effect of different calibration schemes. Dashed line represents same feature for binary fission. Data taken with detectors at 1.5-cm distance from source.

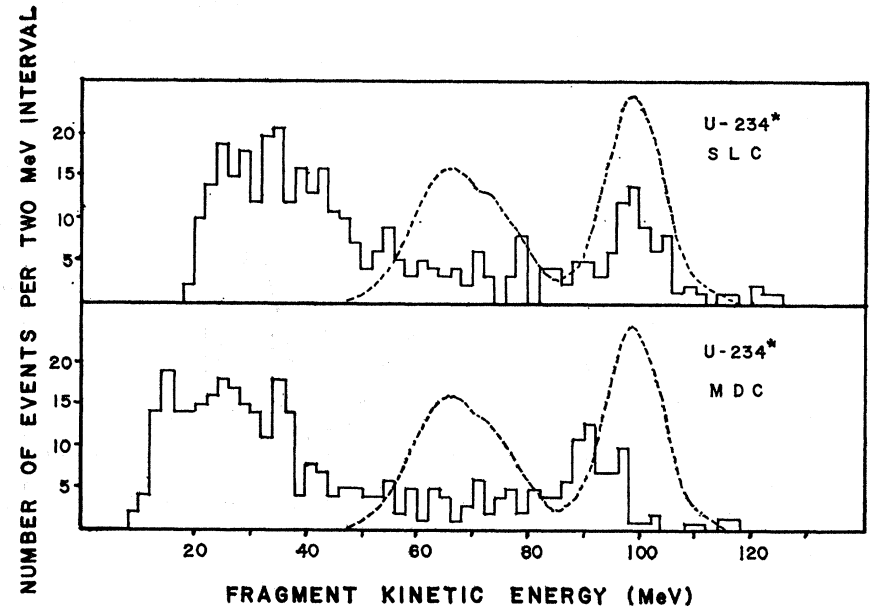

FIG. 6. Single fragment kinetic-energy distribution for U^{234*} system showing effect of different calibration schemes. Dashed line represents same feature for binary fission. Data taken with detectors at 1.5-cm distance from source.

These values have been corrected for the geometrical efficiency[12] of the detectors about the fission source but do not reflect any angular dependency which may exist, and hence should be considered as lower limits.

Some noteworthy features are:

(a) The triple-event count rate (relative to binary fissions) is significantly greater for the U^{234*} (versus U^{236*}) system at the (120-120-120) detector setting.

(b) The ratio is about equal for the two fissioning systems at the other angular settings: (130-100-130), (104-80-140) and (110-140-110). These settings represent arrangements for which scattering events may also be recorded (see Sec. IIIC following).

(c) The effect of reducing the angle subtended is to diminish the relative triple-event count rates, an effect consistent with a more restrictive choice of angles into which the fragments are repelled.

(d) The absolute value of the ratio TF/BF for $U^{235}+n_{th}$ is consistent with previously reported values.[1] (BF = binary fission.)

[12] The factor used is

$$\frac{\pi w \sin\theta}{4(L^2+\frac{1}{4}w^2)^{\frac{1}{2}}[\arctan(w/2L)]^2}$$

which for small values of w/L approximates to $(\pi L/w)\sin\theta$, where L is the distance from the center of the detector to the source, w is the width of a square detector, and θ is the angle between the detector, source, and the symmetry axis.

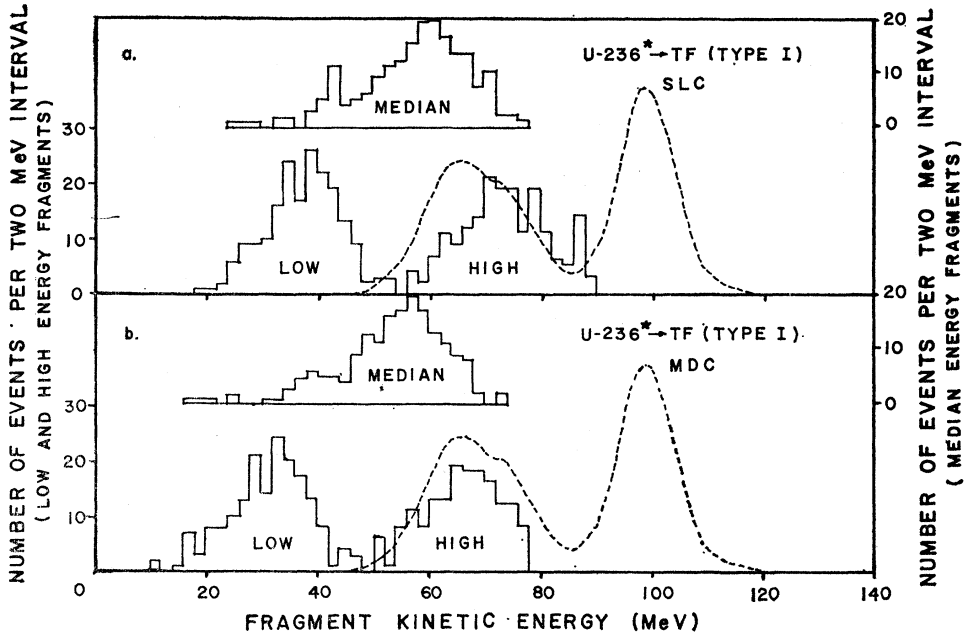

FIG. 7. Single fragment kinetic-energy distribution for type I events for U^{236*} system using (a) straight-line calibration and (b) mass-dependent calibration. Dashed line is for binary fission. Data taken with detectors at 1.5-cm distance from source.

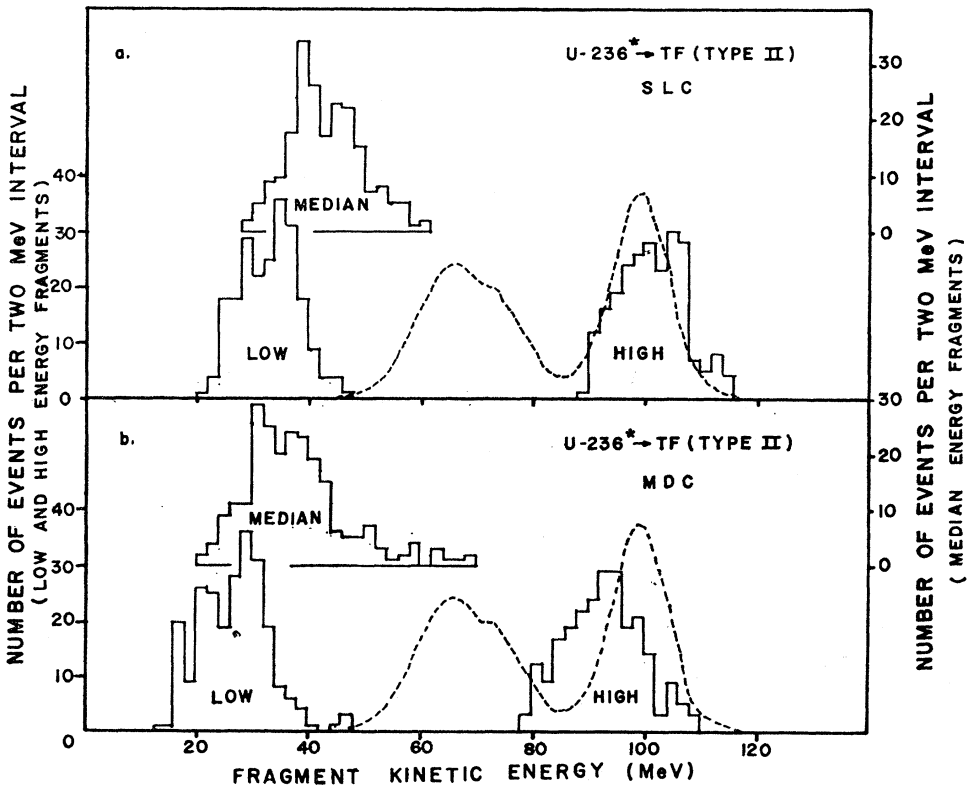

FIG. 8. Single fragment kinetic-energy distribution for type II events for U^{236*} system using (a) straight line calibration and (b) mass-dependent calibration. Dashed line is for binary fission. Data taken with detectors at 1.5-cm distance from source.

B. Origin of the Triple Events

In a three-parameter experiment of this type, one must consider in detail all possible phenomena and/or effects which can give rise to triple events. We list such possibilities as follows: (a) accidental events, (b) instrumental effects, (c) scattering phenomena, (d) ternary fission, and (e) other, e.g., fission with α-particle emission, cosmic-ray showers.

(a) Accidental events—The accidental count rate caused by three independent binary-fission events

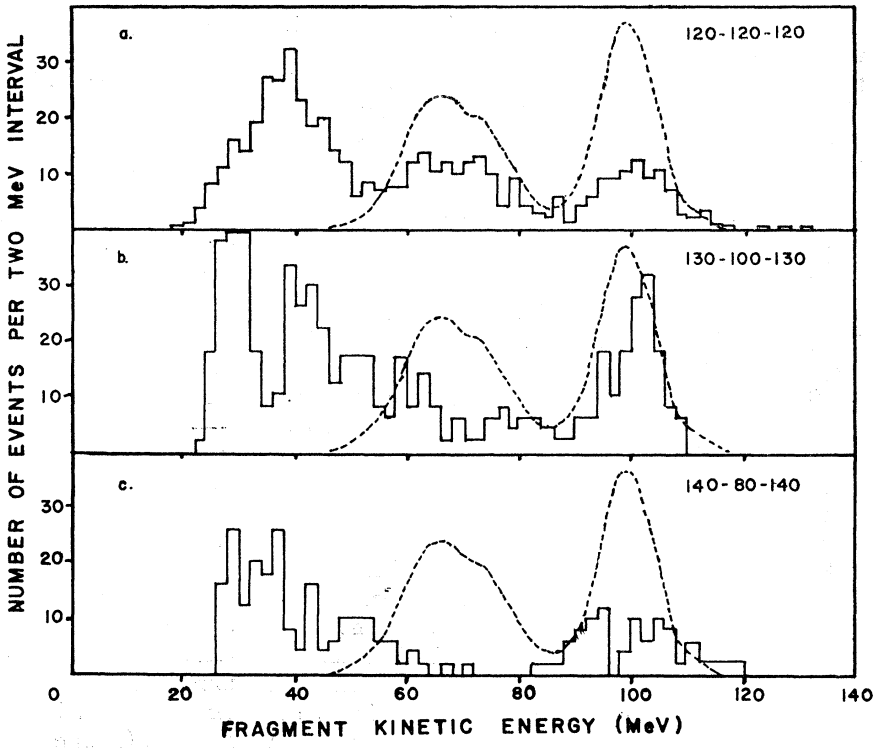

FIG. 9. Single fragment kinetic-energy distribution for the U^{236*} system as a function of angular position (see Fig. 12). (a) 120-120-120, (b) 130-110-130, (c) 140-80-140. Straight line calibration is used. Data taken with detectors at 1.5-cm distance from source. Dashed line is for binary fission.

(triple-coincidence) can be calculated from the following relation:

$$R_{123}=3R_1R_2R_3\tau^2 \quad (1)$$

where R_1, R_2, R_3 are single count rates of the three detectors and τ is the coincidence resolution time. Using some very liberal values of $R=5000$ counts/sec and $\tau=20$ nsec, the accidental count rate is determined to be 1.4×10^{-4}/sec or roughly one accidental count every 2 h. Since, typically, for such a high singles count rate we would observe ten or so triple-event counts per hour, only a small portion of the data can rightly be attributed to accidental events.

Another type of accidental event (binary, single, coincidence) that could possibly trigger all three detectors within the triple-coincidence resolving time is described as follows: If, due to some reason (e.g., carry-over of the fissile material to the detector face or "overlap" of the fission source by the extreme edges of any two detectors) a single binary-fission event could trigger two detectors at the instant that a second binary-fission fragment impinged on the third detector, then a triple event would be recorded.

In such a case the binary count rate (coincidence between two detectors) would necessarily have to be much greater than that expected from two individual but coincidental fragments (in order to account for the observed triple-event frequency). In fact, however, the double-coincidence count rate (between any two detectors) was observed to be consistent with that expected for independent binary accidental events as given by the relation

$$R_{12}=2\tau R_1R_2. \quad (2)$$

A more powerful argument against accidentals appears in the total fragment kinetic-energy spectrum to be expected. Three independent binary-fission fragments should produce a kinetic-energy sum roughly 50% greater than that observed in binary fission i.e., one would expect broad peaks analogous to sum peaks obtained in γ-ray scintillation spectroscopy. Indeed it is just this signature which is used to discard a very few triple events believed to be due to accidentals i.e., those having total kinetic energies substantially larger than that of binary fission. (See Fig. 4 of Ref. 3 and text accompanying.)

The nondependence of the triple-event count rate on the singles count rate has already been reported.[2,3] The (triple-coincidence) accidental count rate would be expected to have a linear dependence on the square of the singles count rate.

In other experiments the fast timing signal on one of the three detectors was delayed or advanced beyond the resolution time of the triple-coincidence unit. In all such instances, cessation of the triple events resulted. Since accidental events should not depend on the time alignment, we have here additional evidence against acidental events.

Still another approach to determine the extent of contribution from accidental events involved effectively removing one detector out of the plane defined by the

source and the other two detectors. This noncoplanarity was achieved in practice by raising the source above the plane of the three detectors as diagrammed in Fig. 10. When the source was in the plane, events were recorded; when out of the plane, no events were registered over equal time spans. If the data recorded were due to accidental events (of either type) removal of the source from a coplanar position should have little effect on the triple-event count rate.

All things considered, we find no evidence to suppose that more than just a small fraction (and these easily identified) of the triple-events recorded result from accidental counts.

(b) Instrumental effects—We also checked the proper functioning of our data-recording system. Apart from this, however, many of the observed features which eliminate accidental events from consideration also argue effectively against instrumental effects as contributing to the recorded data.

For example, the experimental modification in which the fission source was placed out of the plane of the three detectors (Fig. 10) should have had no effect on data recorded if these were caused by instrumental malfunctioning. Similarly, no angular dependence of the kinetic energy spectra should result (Fig. 9) nor should one expect any dependence of the energy spectra on the fissioning system as has been observed.[13] In short, it is difficult to conceive of an instrument malfunction which would give rise to data having the observed dependency on either the geometrical configuration of the detectors or the fissioning species of the source.

Furthermore, the equipment in question has been used to detect and record the energies of the three particles arising from fission with simultaneous α-particle emission[1]; the main features reported for this process have been clearly reproduced in our laboratory.

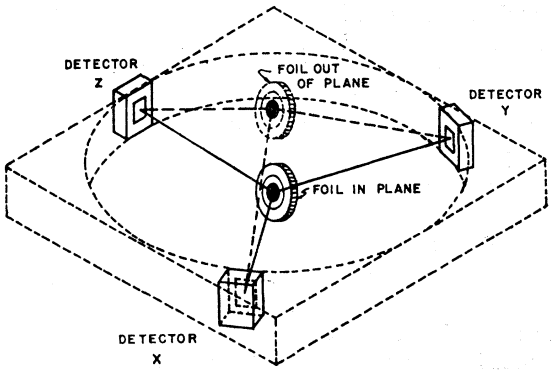

FIG. 10. Schematic diagram of experimental arrangement in which source is removed from plane of detectors. Three-parameter events were observed only when detectors and source were coplanar.

[13] M. L. Muga, C. R. Rice, and W. A. Sedlacek, University of Florida, Nucl. Chem. Rept. ORO-2843-9, 1966 (unpublished); Phys. Rev. Letters 18, 404 (1967).

Finally, in numerous experiments extending over some five years time, the reproducibility of the data for any given set of conditions has been remarkably consistent. There is no indication whatsoever that the data are spurious events caused by instrument malfunctioning.

(c) Scattering phenomena—The possibility of Coulomb scattering is of special importance and is discussed in detail in part IIIC following.

(d) Other—Apart from ternary fission itself, other phenomena which were considered as possibilities to explain the observed data are (a) fission with simultaneous light-particle emission and (b) cosmic-ray showers.

Angular restrictions on the direction of particle emission immediately eliminate the former since the two large fission fragments are repelled approximately 180° apart. The latter explanation, cosmic showers, is equally untenable for a number of reasons, an obvious one being the expectation (not observed) of triple events when reactor power is off.

By a process of elimination we conclude that the only reasonable explanation for the observed data is a fission process in which three large fragments are formed, i.e., ternary fission. The possibility that the ternary fission is induced by fast neutrons and/or α particles (from α accompanied fission) rather than by thermal neutrons seems unlikely in view of the much lower fluxes of these fast particles and their relatively smaller cross sections for interaction.

C. Scattering Analysis

Of all the other possible origins for the observed triple-coincidence events, scattering phenomena are the most difficult to eliminate or to distinguish from ternary fission events. Triple-coincidence events may arise, for example, whenever one fission fragment is scattered by a uranium, fluorine, or carbon nucleus present in the source or backing material, and is then recorded in one detector; the recoil nucleus is ejected into a second detector and the unscattered complementary fission fragment impinges on the third detector.

(a) A theoretical prediction—It is appropriate then to consider the theoretical as well as experimental aspects of this phenomenon in some detail. In the following discussion reference to the presentation of Evans[14] is helpful in understanding some of the expected features of fission-fragment scattering which might be misinterpreted as ternary fission.

Conservation of momentum and energy for these essentially elastic-scattering events requires certain correlations to exist between the fragment scattering angle θ and the angle ϕ of the recoiling nucleus (laboratory system). For the case of a typical heavy- and light-fission fragment scattered by uranium or fluorine nuclei, this correlation is given in the following equation

[14] R. D. Evans, *The Atomic Nucleus*, (McGraw-Hill Book Company, Inc., New York, 1955), p. 828–851.

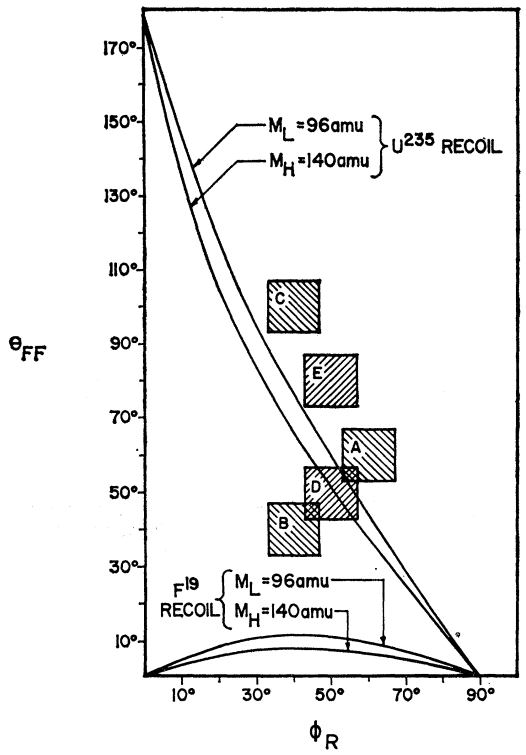

FIG. 11. Correlation between fission-fragment scattering angle and target-recoil angle. See text for explanation.

and is shown graphically in Fig. 11.

$$\cot\theta_{FF}=\frac{M_{FF}}{M_R}\frac{1}{\sin[2\phi_R]}-\cot[2\phi_R]. \quad (3)$$

Subscripts FF and R refer to fission fragment and recoil nucleus, respectively. Two important features that are immediately evident in this plot are stated as follows:

1. Although a uranium nucleus may scatter a fission fragment into any angle in the laboratory system, the uranium nucleus is itself thereby restricted to a definite recoil angle.

2. Scattering of fission fragments by fluorine nuclei involves a maximum scatter angle of about 12°. Inasmuch as the detector arrangements in these experiments do not extend to such small angles(12°), scattering by fluorine nuclei into the detectors is dynamically impossible, hence scattering by fluorine and other light nuclei is not considered further in this analysis.

Next, consider the angular positions of the detectors and the extent of the planar angle which each subtends. For a geometry as shown in Fig. 12(a) ($\alpha=120°$, $\beta=120°$, $\gamma=120°$), a single detector subtending $\pm7°$ will effectively cover the shaded area labeled A on Fig. 11. The additional angular dispersion introduced by the third detector and a nonpoint source is neglected. For this arrangement scattering only of the light fragment would be expected and then would just barely be possible.

For a geometry as shown in Fig. 12(b) ($\alpha=140°$, $\beta=80°$, $\gamma=140°$), the same size detectors will effectively "sweep "two regions B and C, of Fig. 11 corresponding to fragment scattering angles of about 40° and 100°, respectively. In neither case should we expect to detect appreciable scattering events under these conditions (as evidenced by the failure of the detectors to "overlap" the allowed scatter-recoil angles).

For still a third arrangement as shown in Fig. 12(c), ($\alpha=130°$, $\beta=100°$, $\gamma=130°$), the detectors will "sweep" regions D and E of Fig. 11 corresponding to fragment scattering angles of approximately 50° and 80°, respectively. Of these possibilites, a scatter angle of 50° for the heavy fragment accompanied by uranium recoil angle of 50° represents a favorable situation for a scattering event to be recorded, the complementary light fragment emerging undeflected. Scattering of the light fragment appears also to be possible for this detector geometry [Fig. 12(c)].

Assuming such scattering events obey a true Rutherford scattering mechanism,[15] an estimate of the cross section per unit solid angle ($d\sigma/d\Omega$) can be made. Using as input data the typical heavy- and light-fragment masses and velocities, for a UF_4 source foil 100 $\mu g/cm^2$ thick, the fraction of binary fission fragments (both light and heavy) calculated to scatter into the defined geometry of 50° is 10×10^{-6}. This value is not inconsistent with that observed for triple events at this angular setting (130-100-130) (see Table IV). About 85% of these will be heavy-fragment scattering.

Further analysis can be made by considering energy-transfer correlations through elastic collisions. For a

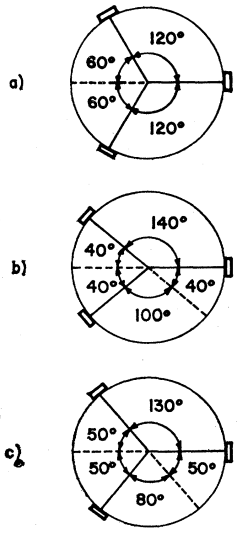

FIG. 12. Angular arrangements for which triple-coincidence events were investigated. (a) 120-120-120 (b) 140-80-140, (c) 130-100-130. As explained in text, only for a configuration such as (c) can scattering events be recorded. This restriction was verified experimentally.

[15] Some deviation from the calculated value of the Coulomb scattering cross section is expected to occur because of the effect of screening of the nuclear charge by the electronic fields about the fission-fragment ions and recoil nuclei.

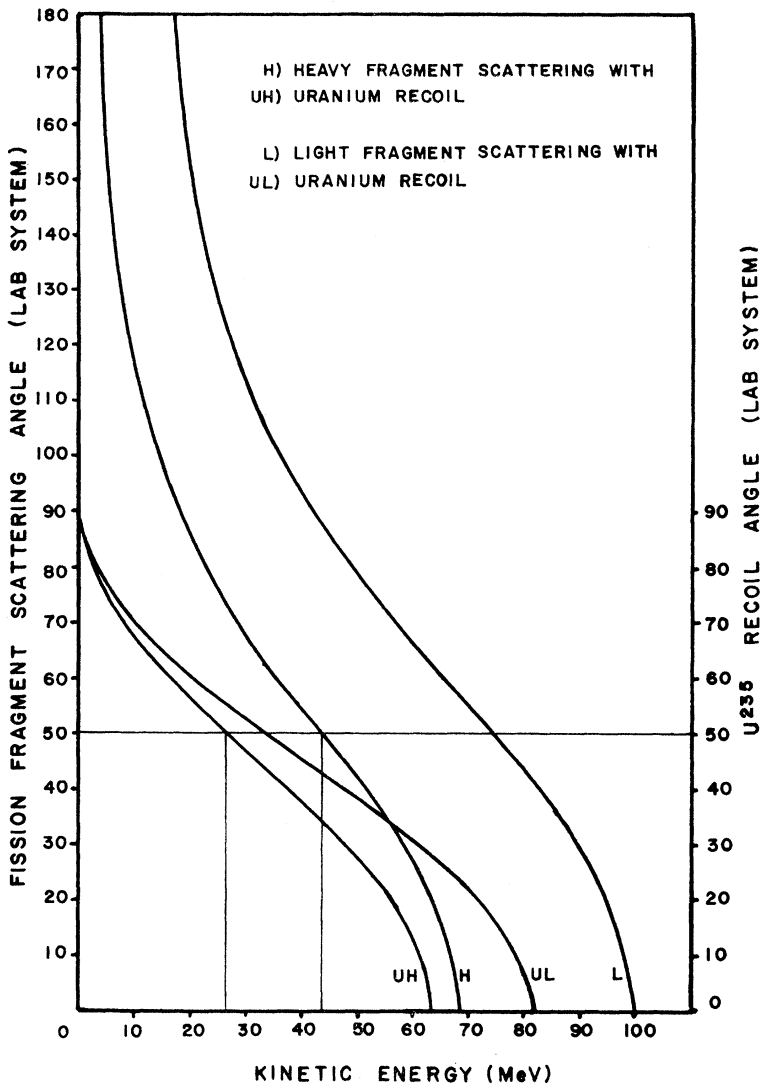

FIG. 13. Energy transfer for elastic collision between typical heavy (140 a.m.u., 68.4 MeV) and light (96 a.m.u., 99.8 MeV) binary-fission fragment with uranium-238 recoil nucleus.

specific combination of scattering and recoil angles (as given by Fig. 11) the energy transfer is fixed (if the fragment mass and initial kinetic energy are considered known). The allowed kinetic energies of the uranium recoil nucleus and scattered fragment as functions of the recoil and scattering angles, respectively, are shown in Fig. 13.

We examine again the features pertinent to the geometrical arrangement of Fig. 12(c) ($\alpha=130°$, $\beta=100°$, $\gamma=130°$). For the case in which a heavy fragment is scattered through 50° (and the uranium recoil angle is 50°), the scattered fragment energy and uranium recoil energy are estimated (from Fig. 13) to be 43 and 26 MeV, respectively. Comparing these values with the energy distributions experimentally obtained at different angular settings, (Fig. 9) it is seen that the predicted peaks (43 and 26 MeV) identify well only with the energy distribution obtained at one specific angular setting, that of Fig. 9(b). In particular, the shape of the energy distribution of Fig. 9(a) ($\alpha=\beta=\gamma=120°$) cannot be resolved with an analysis such as the foregoing.

Briefly then, we have this situation. Of the three geometrical arrangements shown in Figs. 12(a), 12(b), 12(c), only one is expected on theoretical grounds to detect appreciable numbers of scattering events. The energy distributions and frequency of triple events observed experimentally when the detectors are suitably positioned ($\alpha=130, \beta=100, \gamma=130$) are consistent with the explanation that a major portion of these events may result from scattering phenomena. For the other two detector arrangements, however, only a small fraction, if any, can be attributed to scattering phenomena.

(b) Experimental verification—In order to evaluate the contribution to triple events resulting from scattering of fission fragments and in order to verify the foregoing arguments, a scheme was designed to investigate

experimentally the properties of this scattering phenomenon. The detectors and source arrangements are shown in Fig. 14. A collimated beam of fission fragments is allowed to impinge upon an enriched $U^{238}F_4$ foil of known thickness (350 $\mu g/cm^2$); the energies of the scattered fission fragment and recoil uranium atom are recorded by means of two detectors (X and Z) placed at chosen angles about the scattering foil ($U^{238}F_4$); the unscattered complementary fission fragment must be detected simultaneously in the third detector (Y). A three parameter measurement of the binary-fission–scattering event is made. Detectors X and Z are "hidden" from the U^{235} fission source and detect only the scattered fragment and/or the recoil atom; a triple coincidence is required, hence, the unscattered fragment is always recorded by detector Y.

Data were recorded in a manner identical to that described in Sec. II, however, in the data-reduction procedure the mass-dependent calibration was applied differently as follows. The approximate energies were first determined by the straight-line calibration (SLC) method. Of the energies recorded by detectors X and Z, the lower value was associated with the recoil uranium nucleus of mass 238 a.m.u. The other two masses were then determined from momentum conservation laws applied to binary fission fragments.[16] With these masses the mass-dependent calibration (MDC) was used to calculate a new set of energies from which a new set of masses were determined. This latter process was repeated until the energy values converged to within 0.5 MeV.

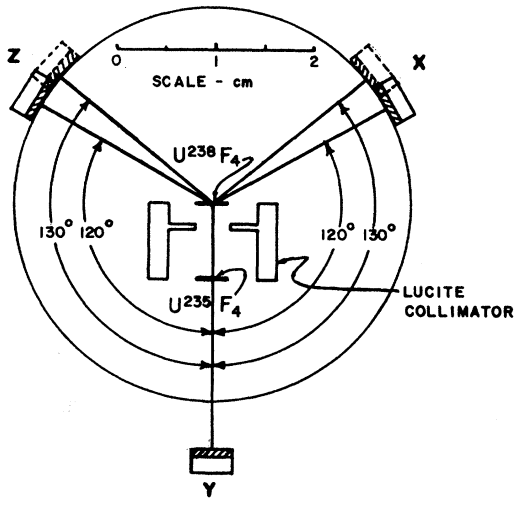

FIG. 14. Scale diagram of experimental arrangement for investigating real fission-fragment scattering.

[16] The relations used are

$$M_1=(E_x+E_z)M/(E_x+E_y+E_z);$$

and $M_2=M-M_1$, where M_1 is the mass of fragment recorded by detector Y, M_2 is the complementary fragment, M is the total mass, and E_x, E_y, E_z are, respectively, the energies recorded in detectors X, Y, and Z.

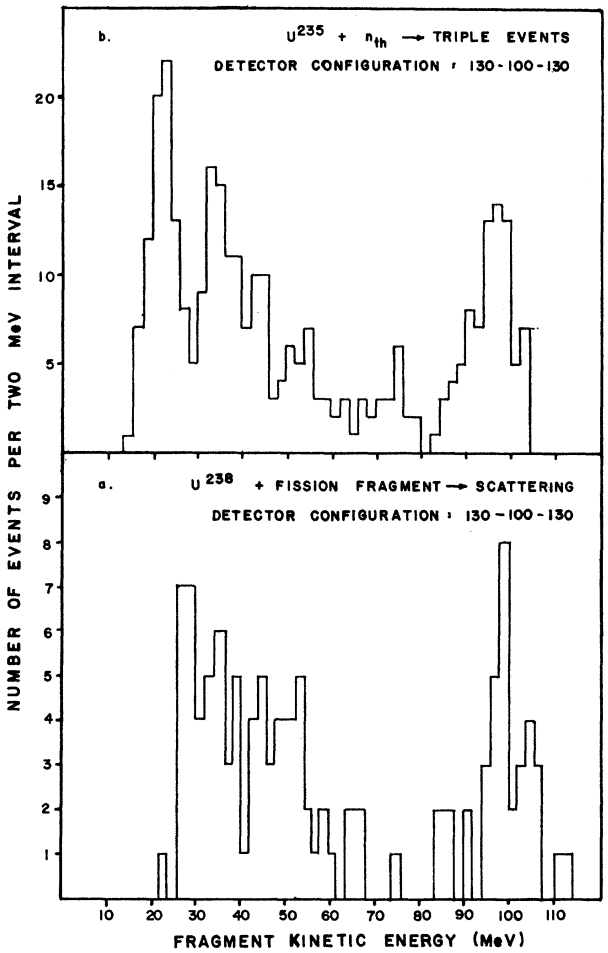

FIG. 15. (a) Single fragment kinetic-energy distribution of binary-fission events (U^{235}+thermal neutron) for which one fragment is scattered in $U^{238}F_4$ foil (see Fig. 14). Angular configuration is 130-100-130. A mass-dependent calibration scheme is used in which one mass (see text) is restricted to 238 a.m.u. (b) Single-fragment kinetic-energy distribution of triple coincidence events from U^{235}+thermal neutron. Angular configuration is 130-100-130. Raw data is identical to that presented in Fig. 9(b); a mass-dependent calibration (MDC) scheme is used in which sum of masses is 236 a.m.u.

As before, experiments were made under the three angular conditions depicted in Figure 12. Scattering events were detected for only one of these settings, namely that of Figure 12(c) ($\alpha=130°$, $\beta=100°$, $\gamma=130°$). The energy-distribution recorded for all three particles is shown in Fig. 15(a) and is seen to be quite similar to that obtained from previous experiments [Fig. 9(b)] at these angles [reproduced in Fig. 15(b)]. The peak positions correspond closely to those predicted on the basis of a scattering analysis. Clearly, a large fraction of these events [Fig. 9(b)] are consistent with a scattering mechanism.

Repeated attempts, however, to record scattering events at the 120° setting [Fig. 12(a)] were unsuccessful. Changing the angles to the 130° setting [Fig. 12(c)] during the same experiment (all other factors remaining

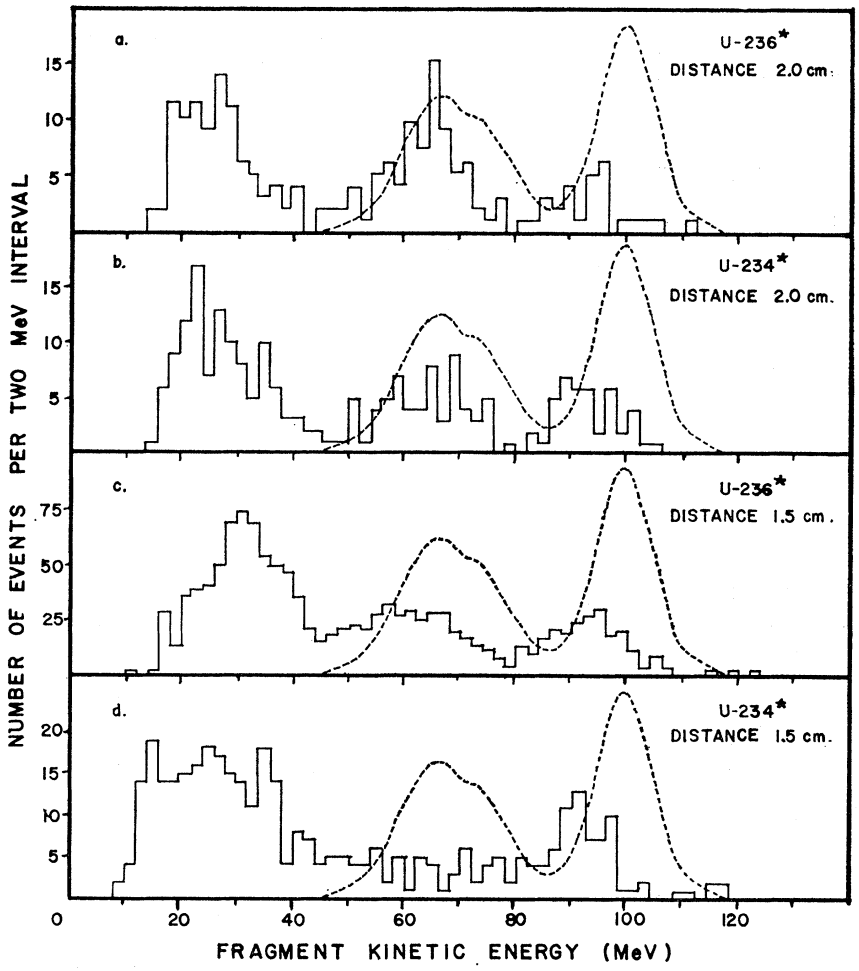

FIG. 16. Comparison of single fragment kinetic-energy distributions from ternary fission of U^{236*} and U^{234*}. (a) U^{236*}, detectors at 2.0 cm distance; (b) U^{234*}, detectors at 2.0 cm distance; (c) U^{236*}, detectors at 1.5-cm distance; (d) U^{234*}, detectors at 1.5-cm distance.

unchanged) gave positive results, thus assuring proper functioning of the equipment.

We conclude on the basis of these experiments that the symmetrical positioning of detectors 120° apart (subtending ±7°) is such that scattering events of binary fission fragments cannot be recorded; all triple events thus recorded must result from another cause.

(c) Other evidence—The nondependence on the source foil thickness of the ratio of the triple-event count rate to the singles count rate has been previously reported[2,3] for the symmetrical detector arrangement ($\alpha=\beta=\gamma=120°$). The scattering cross section should have a linear dependence upon the thickness of the UF_4 film, and will approach zero for an infinitely thin film. On the other hand, the ternary-fission count rate should vary directly *only* with the singles count rate (for a given angular setting), as has been observed.

Another argument against scattering appears in a comparison of the energy distributions of the U^{236*} and U^{234*} systems reproduced in Fig. 16. Since the mass divisions and kinetic energies of the fragments formed in binary fission of these two systems are closely alike, the factors which affect scattering (atomic number, mass and energy of scattered fragment, atomic number and mass of uranium recoil nucleus) are essentially identical. Hence, triple-event data, recorded under identical conditions for these two systems, should be indistinguishable if caused by scattering phenomena. An examination of Fig. 16 shows clearly that the respective energy distributions are quite different; therefore scattering cannot be the explanation. For a fuller account of this approach see Ref. 13.

The data presented to substantiate the arguments of this section were accumulated from multiple series of identical experiments for which consistent and reproducible results were observed.

Summarizing this section, the following arguments indicate the absence of scattering phenomena for the case of a symmetrical detector arrangement ($\alpha=\beta=\gamma=120°\pm7°$).

1. From the dynamics (kinetics) involved it is impossible for the detectors to record a scattering event. The energy distribution and angular dependence predicted are, however, consistent with and at least partly explain the triple coincidence data collected at another angular setting, viz. $\alpha=130°$, $\beta=100°$, $\gamma=130°$.

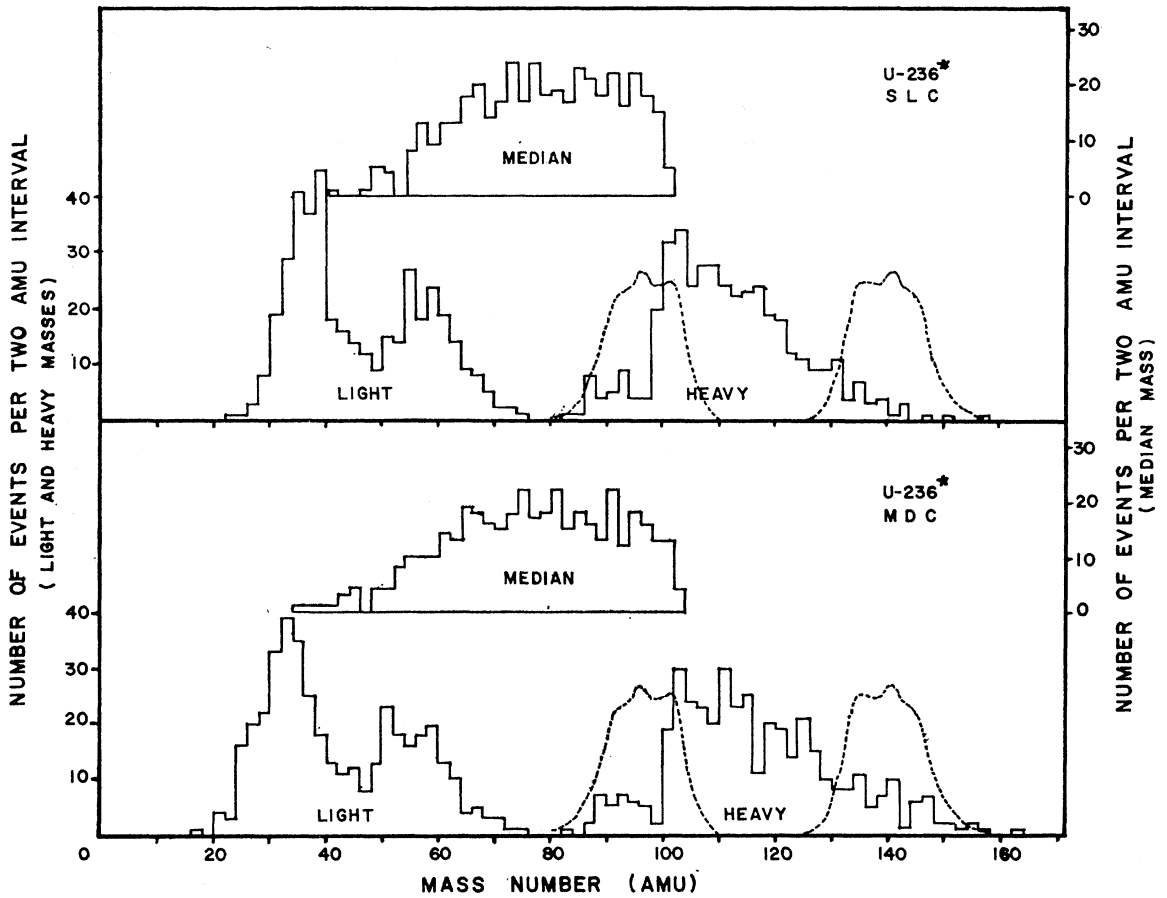

FIG. 17. Fragment-mass distributions for U^{235}+thermal neutron → ternary fission showing effect of different calibration schemes. Dashed line in this and subsequent figures represents binary-fission mass yield (arbitrary scale).

2. The foregoing analysis has been experimentally verified by observing the feature of binary-fission fragment scattering. Neither the energy distribution nor the angular dependence of true scattering events is consistent with or able to explain the data collected at the 120° angles.

3. The ratio of triple events to binary events recorded is independent of the source foil thickness. A linear dependence should be observed if scattering were involved.

4. The energy distributions for U^{236*} and U^{234*} are markedly different; they should be virtually identical if scattering is the correct explanation.

Although these arguments do not by themselves prove the existence of ternary fission, they clearly eliminate scattering phenomena as a possibility.

D. Mass Distributions and Interpretation

In the previous sections, III B and III C, we have presented arguments for excluding effects other than ternary fission as causes of the observed triple events. If we accept the existence of ternary fission, we can proceed to develop what is perhaps the most interesting feature of these data, namely the mass distributions and their implications on fission theory.

Converting the energy data, we obtain the mass distributions shown in Figs. 17 and 18 for the fissioning systems U^{236*} and U^{234*}, respectively. The effect of the mass-dependent calibration scheme is that of shifting the lighter masses to still lower values; application of the quadratic-mass-dependent calibration gives essentially the same distribution as the mass-dependent scheme. In the following presentation we retain only that mass data generated using the mass-dependent calibration (MDC) scheme.

A distinctive feature of the *light* mass fragment distribution is the appearence of two peaks, a lower one near mass 30 and a higher one in the mass range 50–60 a.m.u. In accordance with earlier work[3] we separate the events as to type I or II. Type I includes those events for which the light mass fragment lies near the range 50–60 a.m.u. and type II represents those events for which the light fragment corresponds to the lower peak (near mass 30). A replot showing this delineation is given in Figs. 19 and 20 for the two fissioning systems.

The U^{236*} fissioning system has a higher ratio of type

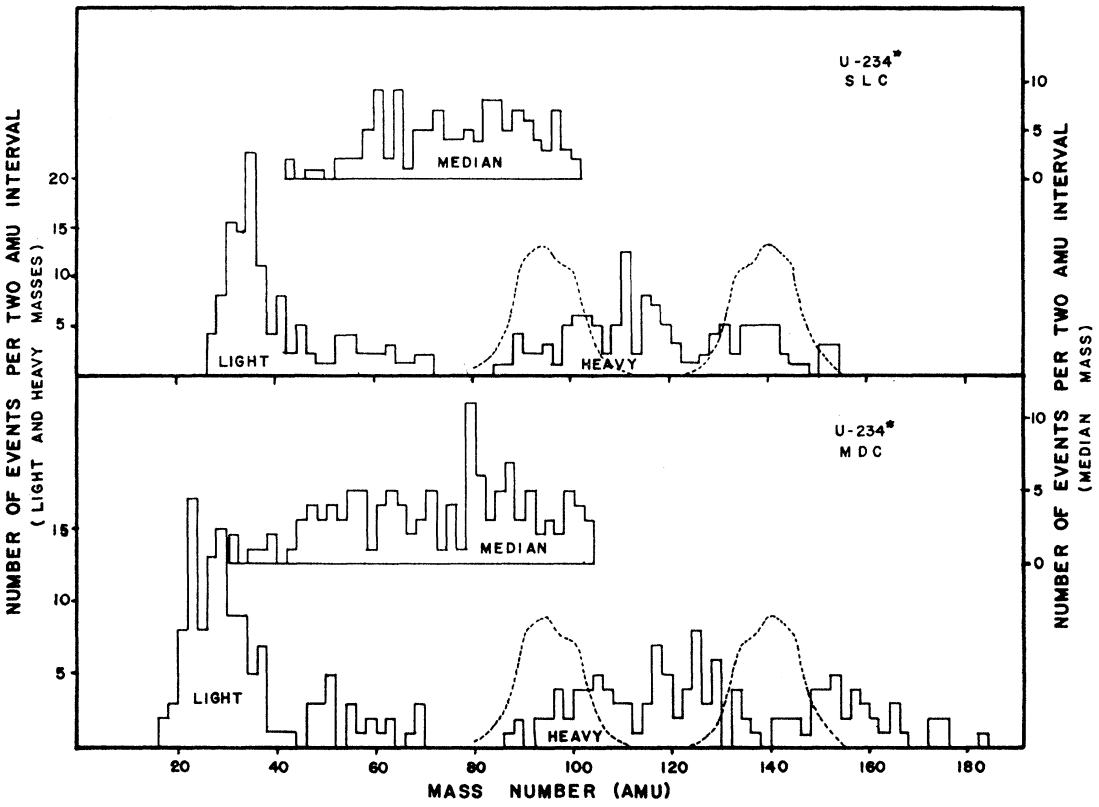

FIG. 18. Fragment-mass distributions for U^{233}+thermal neutron → ternary-fission showing effect of different calibration schemes.

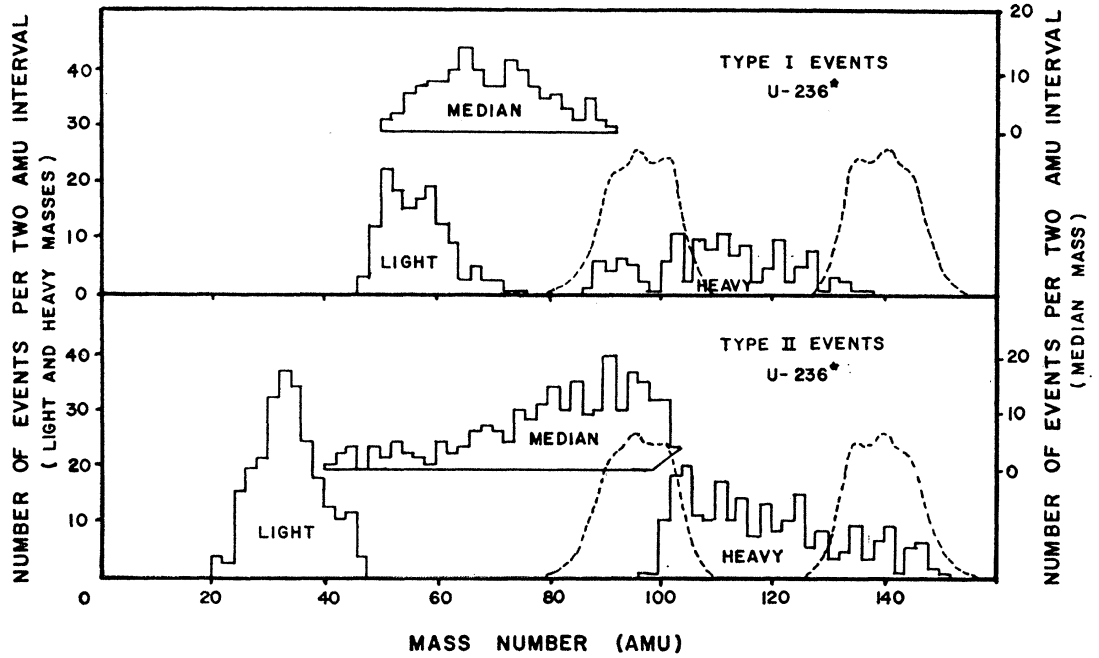

FIG. 19. Fragment-mass distributions of type-I and type-II events from ternary fission of U^{236*}. Mass-dependent calibration used. Detectors at 1.5-cm distance from source.

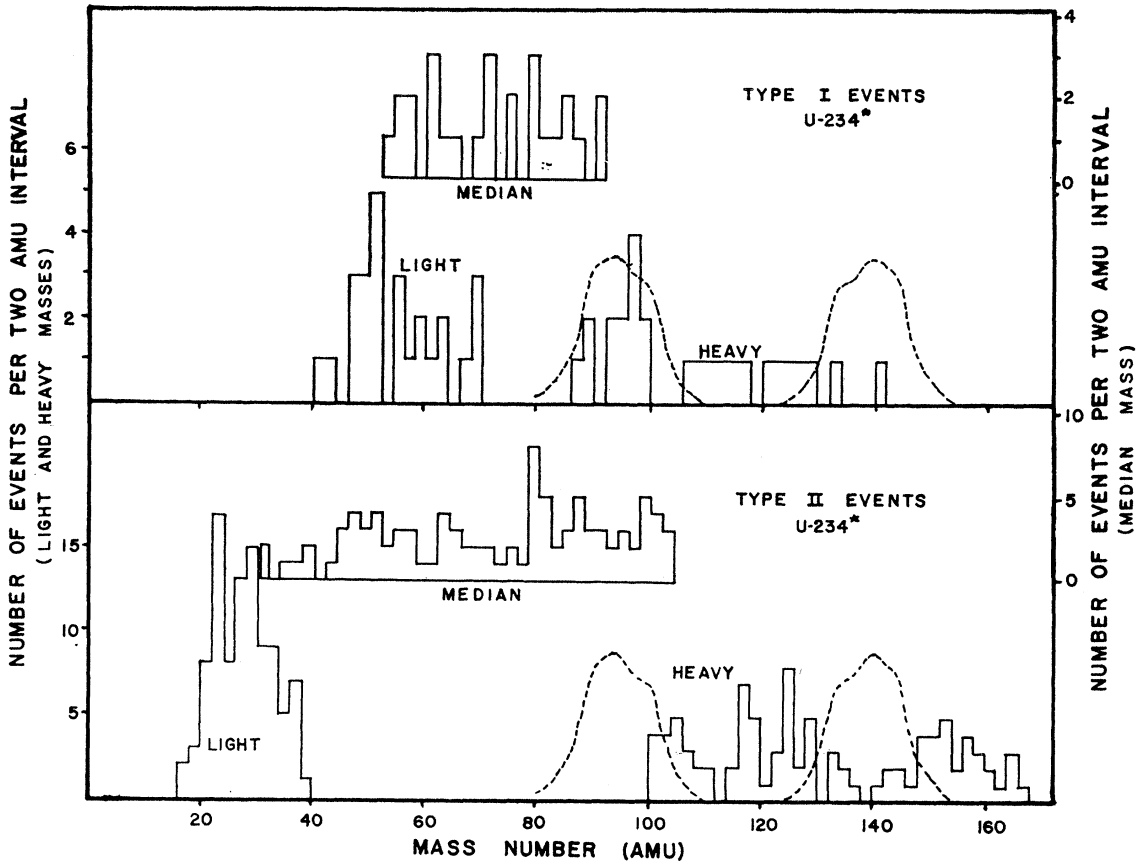

FIG. 20. Fragment-mass distributions of type-I and type-II events from ternary fission of U^{234*}. Mass dependent calibration used. Detectors at 1.5-cm distance from source.

I/type II events compared to U^{234*}. We interpret this distinction as arising from the effect exerted by the two additional neutrons in the U^{236*} system, an effect reflecting the dominance of shell structure in shifting the mass distribution from type II to type I. To elaborate, we view the extra two neutrons as facilitating the formation (within the pre-scission configuration) of the larger (type I) of the two possible light masses, consistent with the general expectation that this larger mass will have a larger value for its stable N/Z ratio. The dominant influence of shell structure opens the possibility of formation of unique masses (perhaps stable) in the ternary fission process.

We can qualitatively support these ideas by citing previous work [8,9,17–19] reporting the existence of fine structure in the kinetic energy distribution of U^{235}, U^{233}, and Pu^{239} binary fission induced by thermal neutrons and Cf^{252} spontaneous binary fission. This fine structure is more apparent when the kinetic energy of the light fragment is large, i.e., when, the gross distortion and subsequent available excitation energy is minimized. It has been suggested[8] that when fission occurs at low excitation energies there is a preferential selection of the generally more stable even-even nuclei, and indeed, Thomas and Vandenbosch[20] have shown that there is a correlation between fine structure and the structure inherent in the mass surface of the product fragments. The ternary fission process may be viewed as an extreme case of this preselection of final product masses. Furthermore the very infrequency of occurrence of ternary fission suggests the availability of a limited number of channels or pathways leading to tripartition, hence the expectation of unique mass formation is not unreasonable.

The effect of the subtended angle on the variation of type I and type II modes is shown in Figs. 21 and 22. The U^{236*} system has a strong angular dependency, increasing in the relative number of type I events as

[17] W. M. Gibson, T. D. Thomas, and G. L. Miller, Phys. Rev. Letters 7, 65 (1961).

[18] W. M. Gibson, T. D. Thomas, and G. Safford, in *Proceedings of the Symposium on the Physics and Chemistry of Fission* (International Atomic Energy Agency, Vienna, 1965), Vol. I, paper SM-60/36, p. 467.

[19] J. C. D. Milton and J. S. Fraser, Phys. Rev. Letters, 7, 67 (1961).

[20] T. D. Thomas and R. Vandenbosch, Phys. Rev. 133, B976 (1964).

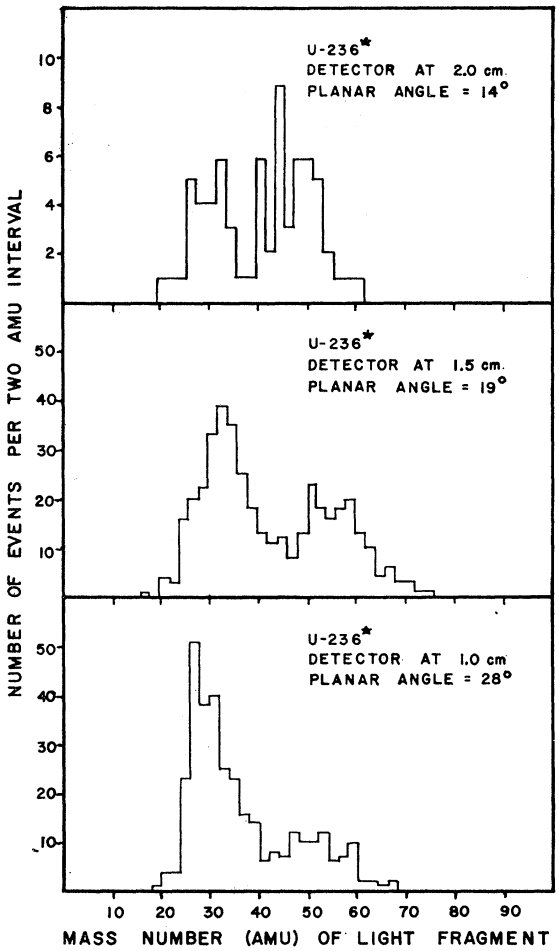

FIG. 21. Light-mass distribution as function of radial position of detector. U^{236*} system.

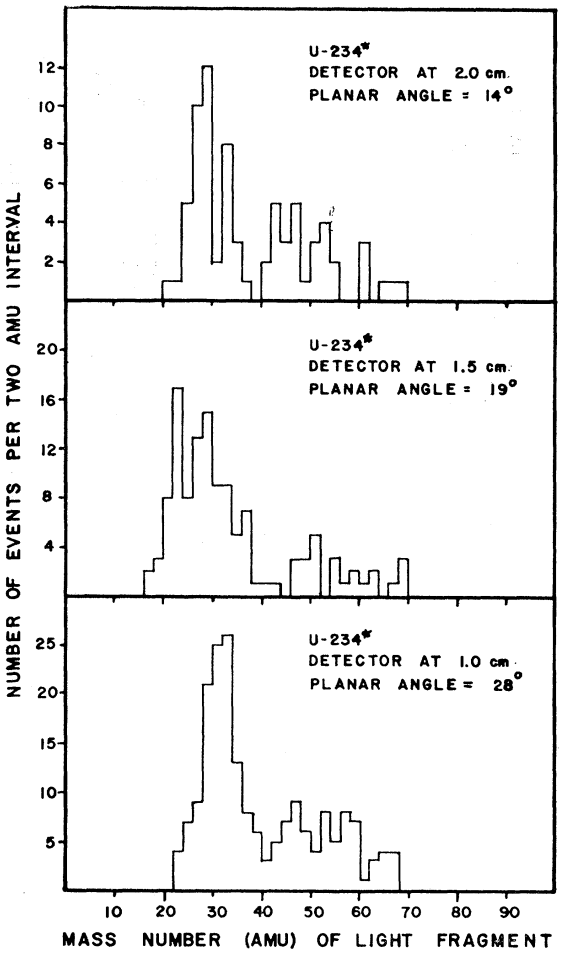

FIG. 22. Light-mass distribution as function of radial position of detector. U^{234*} system.

the angle becomes better defined. The detector configuration is (120-120-120). For the U^{234*} system, the number of type I events relative to type II remains essentially unchanged. Since the over-all mass resolution depends upon four factors (energy resolution, finite size of source, solid angle subtended and fraction of events caused by scattering), improvement of angular resolution *alone* does not suffice to produce significant sharpening of the mass peaks as might otherwise be expected.

The existence of ternary fission in which the fragment masses are repelled at angles 120° apart implies an axially asymmetric distortion at the moment of scission, a configuration not usually considered in fission theory. Dynamically (and qualitatively), we can classify the fission process as involving either a "going away" scission, or a "snapping back" scission.

In the former model, we view the scission as taking place while the yet unformed end fragments are continuously accelerated in generally opposite directions from their common origin. For this case there appears to be no mechanism for producing axially asymmetric configurations, unless we propose, not an initially elongating distortion, but a three-node symmetrical configuration as shown in Fig. 14(c) of Ref. 3. This type of distortion rapidly increases the surface (area) energy without a compensatingly large charge separation and its accompanying decrease in Coulomb energy. As such, the fission barrier is expected to be much higher as energy must be supplied from a source, other than from decreased Coulomb energy, to increase the nuclear surface area. This scheme could, however, explain ternary fission at higher excitation energies.

In the latter model, an initial surge of the end masses to an extreme elongation is followed by a "snapping back"; however, because of the inertial resistance of these end masses, a "necking down" in the middle portion occurs before the nucleus can reassemble into its original nearly spherical form. Scission occurs then, at a time when the end masses are moving back toward each other. If, following an unusually large elongation,

"necking" occurs simultaneously in two different locations of the middle mass portion, we have a mechanism for guiding the middle fragment into an off-axial position. The returning end fragments will cause the middle portion to "pucker out" during a time interval in which the actual scission occurs. Finally, the predominantly backward motion (i.e., toward the origin) of the now separated end fragments ceases, and acceleration of the three fragments away from each other in three different (but coplanar) directions occurs in their mutually repelling Coulomb fields.

In future experiments, we plan to explore in detail the angular dependency of the frequency of occurrence, and of the mass and energy distributions of ternary fission using three position-indicating detectors and a six-parameter multichannel recording system. From data thereby resulting, we expect to reconstruct real scission configurations leading to tripartite division. Hopefully the continued study of ternary fission will develop quantitative as well as novel concepts concerning the fission mechanism.

ACKNOWLEDGMENTS

We wish to express our dependence upon H. E. Taylor and David Burnsed of this laboratory for their skill in maintaining and updating the electronic data recording system. We are indeed grateful to Dr. Elliot Pierce, USAEC, Washington, for his patience and understanding in regards to these experiments.

APPENDIX: CALIBRATION BASED ON A QUADRATIC MASS DEPENDENCE FORMULA

Examination of the causes of the pulse-height defect of heavy ions in solid state detectors has led to the suggestion that this effect should have a quadratic dependence upon the mass of the measured ion. The success of the linear mass-dependent scheme developed by Schmitt *et al.* for the calibration of fission fragments has led us to extend this scheme to include a quadratic mass-dependence in order (possibly) to better represent the energies of lighter fragments from the ternary fission process.

Accordingly, we have assumed an energy dependence as follows:

$$E=(a+a'm+a''m^2)x+b+b'm+b''m^2, \quad \text{(A1)}$$

where E is the energy associated with pulse height x for a fragment of mass number m. The constants a, a' a'', b, b', and b'', are determined by means of Fig. 4 of Ref. 10 using the pulse-height versus energy dependence of the three mass numbers 127, 80, and 4. Using the notation of previous reports we obtain the "universal" energies for these masses corresponding to the pulse heights (P_L and P_H, respectively) of light- and heavy-mass fragments from binary fission. Using the six conditions imposed by this information the values of the constants in Eq. (A1) are obtained. Results are tabulated in Table V.

TABLE V. Constants evaluated for quadratic mass-dependence formula.

	U^{235}	U^{233}	Cf^{252}
$E_{L,127}$	104.944	105.676	107.01
$E_{L,80}$	98.623	99.315	100.57
$E_{L,4}$	90.15	90.85	92.10
$E_{H,127}$	68.134	67.129	78.45
$E_{H,80}$	63.972	63.036	73.69
$E_{H,4}$	56.00	55.10	65.55
a	$34.226/(P_L-P_H)$	$35.830/(P_L-P_H)$	$26.614/(P_L-P_H)$
a'	$-0.0203/(P_L-P_H)$	$-0.0212/(P_L-P_H)$	$-0.0171/(P_L-P_H)$
a''	$0.000320/(P_L-P_H)$	$0.000336/(P_L-P_H)$	$0.000255/(P_L-P_H)$
b	$89.764-aP_L$	$90.467-aP_L$	$91.721-aP_L$
b'	$0.0958-a'P_L$	$0.0950-a'P_L$	$0.0940-a'P_L$
b''	$0.000187-a''P_L$	$0.000195-a''P_L$	$0.000208-a''P_L$